The Journal of Experimental Biology 209, 3758-3765
Published by The Company of Biologists 2006
doi:10.1242/jeb.02431

The spectral sensitivity of the lens eyes of a box jellyfish, *Tripedalia cystophora* (Conant)

Melissa M. Coates[1,*], Anders Garm[2], Jamie C. Theobald[2], Stuart H. Thompson[1] and Dan-Eric Nilsson[2]

[1]*Hopkins Marine Station, Department of Biological Sciences, Stanford University, Oceanview Boulevard, Pacific Grove, California, 93950, USA and* [2]*Department of Cell and Organism Biology, Lund University, Zoology Building, Helgonavägen 3, S-223 62 Lund, Sweden*

*Author for correspondence at present address: Department of Cell and Organism Biology, Lund University, Zoology Building, Helgonavägen 3, S-223 62 Lund, Sweden (e-mail: Melissa.Coates@cob.lu.se)

Accepted 5 July 2006

Summary

Box jellyfish, or cubomedusae (class Cubozoa), are unique among the Cnidaria in possessing lens eyes similar in morphology to those of vertebrates and cephalopods. Although these eyes were described over 100 years ago, there has been no work done on their electrophysiological responses to light. We used an electroretinogram (ERG) technique to measure spectral sensitivity of the lens eyes of the Caribbean species *Tripedalia cystophora*. The cubomedusae have two kinds of lens eyes, the lower and upper lens eyes. We found that both lens eye types have similar spectral sensitivities, which likely result from the presence of a single receptor type containing a single opsin. The peak sensitivity is to blue–green light. Visual pigment template fits indicate a vitamin A-1 based opsin with peak sensitivity near 500 nm for both eye types.

Supplementary material available online at
http://jeb.biologists.org/cgi/content/full/209/19/3758/DC1

Key words: vision, eye, electrophysiology, electroretinogram (ERG), photoreceptor, opsins, spectral sensitivity, invertebrate, Cnidaria, Cubozoa.

Introduction

Most jellyfish are pelagic drifters, living in the open ocean. However, medusae of the class Cubozoa are neritic; they live near the shore, often in kelp forests or mangrove swamps (for a review, see Coates, 2003). Cubozoans possess remarkable eyes located on sensory clubs called rhopalia. Four rhopalia line the bell of a cubomedusa, and each rhopalium houses six eyes (Fig. 1). Of the 24 eyes (in total) there are four morphologically distinct types. Situated on each rhopalium are a pair of pit ocelli, a pair of slit ocelli, and two unpaired lens eyes; historically the lens eyes are referred to as the large and small complex eyes, but here called simply the lower and upper lens eyes, respectively. A cornea, a cellular lens and a retina of ciliated photoreceptors make up these eyes (Berger, 1898; Yamasu and Yoshida, 1976; Laska and Hündgen, 1982; Nilsson et al., 2005). Unlike vertebrate photoreceptors, the outer receptor segments of cubomedusae photoreceptors face the lens (Yamasu and Yoshida, 1976; Laska and Hündgen, 1982).

One species, *Tripedalia cystophora*, is found near La Parguera, Puerto Rico, among mangrove roots but never in the open mangrove channels. A medusa able to exploit this habitat effectively will gain several advantages. Mangrove swamps are highly productive ecosystems, with reliable food sources and a sheltered habitat. Here *T. cystophora* feed on swarms of the copepod, *Dioithona oculata*, which congregate in light shafts created by the mangrove canopy (Buskey, 2003).

The narrow and complex geometry of the root systems is complicated to navigate. Further, currents due to tides, wind, and rain, flow continually through the root systems, creating a potentially treacherous environment. The tissues of jellyfish are in general extremely fragile and susceptible to scraping and tearing by solid objects (Greve, 1968; Raskoff et al., 2003). It is common to see other jellyfish species impaled after drifting into the mangrove roots (M.M.C., personal observation). Jellyfish like *Tripedalia cystophora*, which exploit this ecological niche, need to protect themselves from abrasion by obstacles while maintaining their location in this habitat. This is possible since they are very strong swimmers (Buskey, 2003), but vision likely plays an important role in this ability (see supplementary material for a video of *T. cystophora* navigating their mangrove environment).

We recently examined the spatial resolving power of the lens eyes (Nilsson et al., 2005), but their functions are still a matter of debate. The existence of these lens eyes has been known for a long time (Claus, 1878) and their function has been the

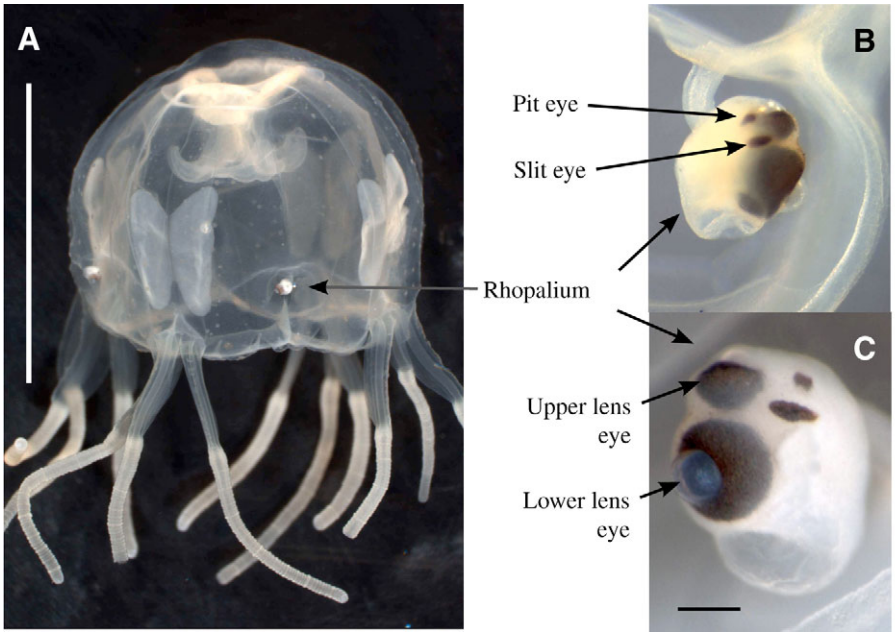

Fig. 1. (A) Photograph of *Tripedalia cystophora*. There are four rhopalia located on the sides of the bell (arrow), which alternate with the four groups of tentacles at the corners. The lens eyes point inward, toward the center of the bell. Scale bar, 1 cm. (B) A photograph of a single rhopalium inside the rhopalial niche. Arrows indicate a pit eye and a slit eye. The slit and pit eyes are both identically matched on the other side of the rhopalium. (C) A photograph of an isolated rhopalium. Arrows indicate the upper and lower lens eyes. Scale bar, 200 μm.

subject of considerable speculation (Pearse and Pearse, 1978; Piatigorsky et al., 1989; Mackie, 1999). Only a few tests have measured the involvement of vision in cubomedusan behavior (Berger, 1900; Hamner et al., 1995; Stewart, 1996). Martin found immunoreactivity to three zebra-fish opsins in the eyes of cubomedusae (Martin, 2004). This indication of three different opsins is very interesting, since it would offer the possibility of color vision in the cubomedusae. Color vision itself implies a level of complexity of the visual tasks performed by an animal. Some visual tasks, such as motion detection, are thought to be color-blind even in organisms possessing color vision (Livingstone and Huebel, 1986), while others, such as object recognition or judging a certain quality of an object, are often impossible without color discrimination. Therefore, determining the possible state of color vision in these organisms gives investigators a selection of visual tasks to explore when trying to determine the functions of the lens eyes. Addressing this question using antibodies against zebra-fish opsins has some weaknesses, since the specificity of an antibody from such a distant relative is doubtful at best (Parkefelt et al., 2005). Further investigation is therefore necessary before conclusions can be drawn about the spectral sensitivity and possible array of visual tasks of these organisms.

Here we use electroretinograms (ERGs) to measure the spectral sensitivity of both the lower and upper eyes, of the Caribbean species *Tripedalia cystophora*, using suction electrodes. This gives a more direct measure of the number and type of photopigments present in the eyes of cubomedusae.

Materials and methods

Animals

Experimental animals *Tripedalia cystophora* (Conant) came from a laboratory colony of La Parguera, Puerto Rico descendants [established at Hopkins Marine Station by M.M.C. (Coates, 2005)]. We used adult male and female medusae ranging in size from 5 mm to 12 mm in bell diameter. We maintained laboratory animals at 25–29°C, in flowing seawater, filtered nominally to 5 μm. Room light cycled on a 14 h:10 h light:dark program. Medusae fed on San Francisco strain *Artemia nauplii*, SELCO (Self Emulsifying Liquid Concentrate) enriched for 24 h post-hatching (Brine Shrimp Direct, Ogden, UT, USA).

Electrophysiological techniques

We stimulated the intact lens eyes of isolated rhopalia with light that varied in intensity and wavelength. Extracellular glass suction electrodes (5–20 μm tip i.d.), placed where the pigmented photoreceptors come closest to the rhopalial surface, recorded field potentials from the retina (ERGs). A P55 A.C. pre-amplifier (1000x, Grass Instrument Company, W. Warwick, RI, USA) fed the signal to a data acquisition board (PCI-6024E, National Instruments, Austin, TX, USA) at 5000 samples s^{-1} (Hz), linked to a computer running specialized software made with LabView (National Instruments). The signal passed through a high-pass filter (cut-off 0.3 Hz) and a low-pass filter (cut-off 0.1 kHz) in the pre-amplifier and a Humbug 50 Hz noise eliminator (Quest Scientific, North Vancouver, BC, Canada) on the way to the data acquisition board.

Isolated rhopalia were dark adapted for a minimum of 30 min prior to stimulus exposure. The stimulus flashed for 40 ms, and recordings lasted 6.0 s with the flash appearing after 1.5 s (Fig. 2). All recordings were followed by a 10.0 s rest to allow recovery from light adaptation induced by the flash. An ophthalmoscope (Nilsson and Howard, 1989) controlled the delivery of a light beam from a xenon arc lamp (Oriel, Darmstadt, Germany), approximately 70–150 μm in diameter

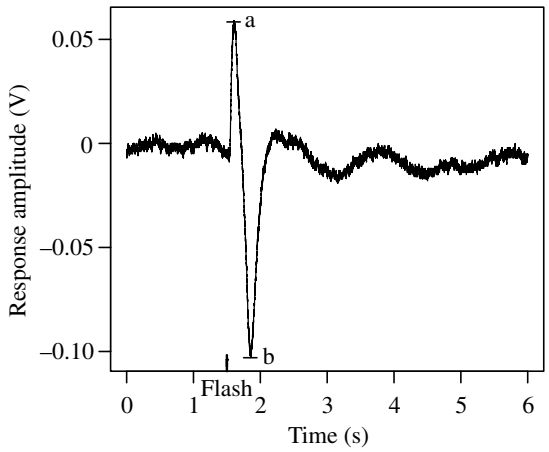

Fig. 2. A sample ERG trace showing the response of an isolated rhopalia to a flash of white light, 40 ms in duration, at 5.47×10^{3} W m^{-2} sr^{-1} (ND 0.5). Peak response is taken as first peak (a), regardless of polarity. It is assumed that the first response is from photoreceptors and subsequent peaks (b) may be from downstream events.

at the surface of the rhopalium (actual size adjusted to fill the diameter of the lens being stimulated). This beam illuminated the lens of interest only, ensuring the response recorded originated in that eye.

Extracellular recordings do not determine whether photoreceptors hyperpolarize or depolarize, as the polarity of the measured response changes with electrode placement. We took the first peak, regardless of polarity, to be the response from the photoreceptors. Any further peaks were assumed to result from downstream events, but as these were inconsistent, we performed no analyses on them.

V–logI recordings

We varied the light intensity with quartz neutral density (ND) filters (Melles Griot, New York, NY, USA) over 4.0 log units in steps of 0.5: (1.73–1.73×10^{4} W m^{-2} sr^{-1}), as measured by an IL 1700 research radiometer (International Light, Inc., Newburyport, MA, USA). Ultraviolet and infrared block filters (Schott, Mainz, Germany) ensured delivery of white light between 420–700 nm. Typical daytime irradiance in bright sunlight is 10^{20} photons s^{-1} sr^{-1} m^{-2} (Land, 1981) and here our maximum intensity was 5.64×10^{17}. Although our stimulus may be 1–3 orders of magnitude less than the brightest intensities encountered by *Tripedalia cystophora* in a light shaft, it was sufficient to trigger photopic vision.

Experiments ran from low to high intensity. At each intensity we averaged the response to 5–30 flashes, according to the health and signal-to-noise ratio of each preparation. This was a compromise between stability and noise – how long the preparation would stay healthy and how many trials were necessary to acquire a clean signal. *V*–logI (voltage *vs* log of intensity) curves were measured before and after presentation of a series of colored flashes and then used in the calculation of spectral sensitivity by converting the stimulus intensity at each wavelength to an equivalent intensity of white light (see below).

The resulting *V*–logI curves were also normalized, and combined to form a mean *V*–logI curve. In total, 14 lower and 8 upper eyes each were subjected to the full range of stimuli.

Spectral sensitivity recordings

The stimulus wavelength varied from 350 to 710 nm, in 30 nm steps, using interference filters whose band-pass at half-maximum transmission was ±10 nm (Melles Griot). Two layers of polarizing film (Polaroid, Waltham, MA, USA) created crossed polarizers, the density of which could be adjusted by rotating, to ensure equal quanta stimulation at all wavelengths.

The *V*–logI curves enabled us to calculate spectral sensitivity from the response measured at each wavelength. We averaged *V*–logI curves taken before and after the spectral measurements. We used the Nedler–Mead optimization function to fit a sigmoid to the resulting *V*–logI curve (Fig. 3):

$$F(x) = b + \frac{(t–b)}{1+10^{(\mathrm{i}–x)s}}\,. \qquad (1)$$

Here b, t and s are the lower bound, upper bound, and slope of the sigmoid, and i is the intensity of the 50% response. We chose a sigmoid curve because it follows constraints similar to those we expect from the biological responses; specifically, a retina's response approaches zero at low intensities, a saturated maximum at high intensities, and varies in between. Further, sigmoids are invertible; swapping the independent and dependent variables yields a proper function:

$$F(y) = i - \frac{1}{s}\log_{10}\left(\frac{(t–b)}{y–b} - 1\right). \qquad (2)$$

With the inverse sigmoid fit for a preparation, we converted the stimulus intensity at each wavelength to an equivalent intensity (i) of white light. This gives sensitivity (S) according to the following equation:

$$S = 100\times10^{\mathrm{i}–\max(\mathrm{i})}\,. \qquad (3)$$

A final spectral sensitivity curve, ± s.e.m. (standard error of the mean), resulted from the average of all sensitivity curves of a given eye type.

Results

The ERG responses of both eye types to light stimuli in *Tripedalia cystophora* consisted of graded receptor potentials. Since the recordings were performed with extracellular electrodes it is not known whether the receptors respond with depolarization or hyperpolarization. The initial response amplitude could be positive or negative independent of eye type. The responses were usually biphasic, the second peak having the opposite polarity of the first (Fig. 4). In a preparation that gave very strong responses, the response could become monophasic at the highest intensities (data not shown). Again,

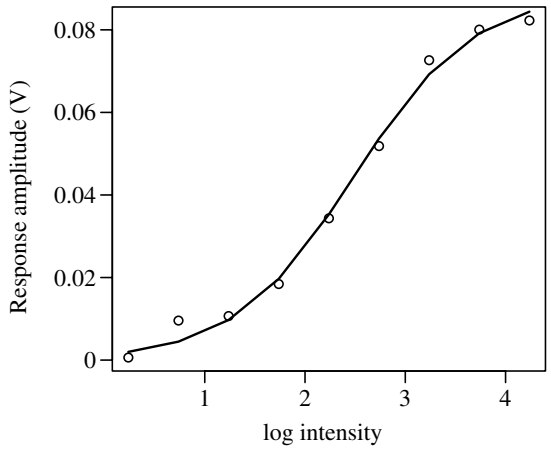

Fig. 3. A single *V*–logI curve from a lower lens eye. Data points (open circles) show how the response changed with changing light intensity (I; W m^{-2} sr^{-1}), while the model fit (solid line) shows the sigmoid shape of this response. For each preparation the *V*–logI-based model fit was used to calculate spectral sensitivity for that preparation (see text for details).

because the second phase was inconsistent, all of our analysis focused on the first peak of the response. Differences in polarity are likely due to the nature of extracellular recordings and differences in electrode placement. Differences in the number of phases may result from the photoreceptors themselves, or from higher order neurons. In these ERGs several receptor cells are contributing to the response in one recording. There were no differences seen in the response characteristics between the two types of lens eyes.

The *V*–logI curves show that both eye types responded dynamically over 3 log units of intensity. Both lens eyes responded measurably to stimuli as dim as 1.73×10^{1} W m^{-2} sr^{-1}. Their response amplitudes increased with brighter light over a range of 3 log units (Fig. 5). The photoreceptor responses, however, did not saturate over these intensities and it is likely that the response range is broader than measured here.

In the course of measuring spectral sensitivity we determined that the lens eyes are not sensitive to the plane of polarization of the light stimulus. This result is implied by previous anatomical work (Laska and Hündgen, 1982), which shows a more or less random arrangement of the assumed photopigment-containing microvilli.

The lower lens eye spectral sensitivity curve peaks in the blue–green region near 500 nm (Fig. 6, solid line). The width of the curve at half-maximum sensitivity (half-width) is 107 nm. The sensitivity falls to 10% of the maximum at 395 nm on the short wavelength tail and 614 nm on the long wavelength tail of the curve. The results are very similar in the upper lens eye, which also peaks near 500 nm (Fig. 6, broken line). Here the half-width is 112 nm. On the short wavelength end of the spectrum the upper lens eye reaches 10% of the maximum sensitivity at 370 nm while on the long wavelength end this is reached at 661 nm. These values are measured from the data points simply by interpolating a curve that connects the points with lines. Plotting on the same graph shows the similarity in shape and peak of the two sensitivity curves (Fig. 6).

Spectral sensitivity curves are well modeled by both the Stavenga-Smits-Hoenders (SSH) rhodopsin template (Stavenga et al., 1993) and the Govardovskii-Fyhrquist-Reuter-Kuzmin-Donner template described [(Govardovskii et al., 2000), here abbreviated as GFRKD] using a Nelder–Mead non-linear optimization (Fig. 7). For the lower eye the models give α-peak absorbances of 498 nm (SSH) and 496 nm (GFRKD). Although neither model can fit a β-peak to the data both produce similar correlations (0.927, SSH; 0.903, GFRKD). For the upper eye models yield peaks of 496 nm

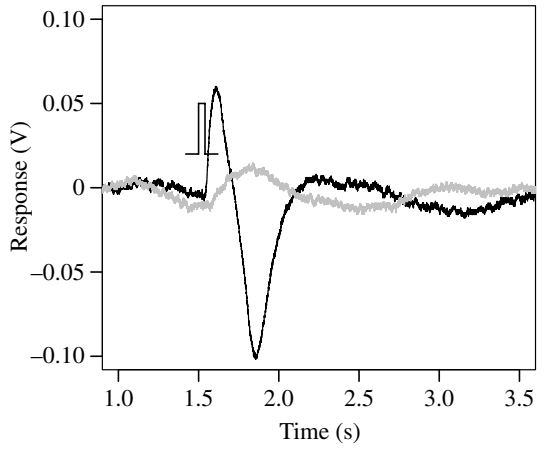

Fig. 4. Response characteristics change with intensity of the stimulus. Here, an ERG trace showing the response to a flash of white light at 5.47×10^{3} W m^{-2} sr^{-1} (ND 0.5, black trace) is noticeably biphasic. However, when the same preparation was stimulated by a much lower intensity (1.73×10^{1} W m^{-2} sr^{-1} , ND 3.0), the response appears more monophasic and is of smaller magnitude (gray trace). Inset shows onset (1.5 s) and duration (40 ms) of flash.

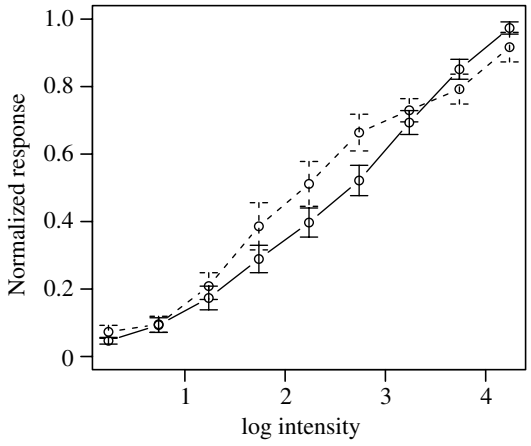

Fig. 5. Normalized response *versus* stimulus intensity (W m^{-2} sr^{-1}) for the lower and upper eyes (*V*–logI). Values are means ± 1 s.e.m. Solid line, lower eye (*N*=14); broken line, upper eye (*N*=8).

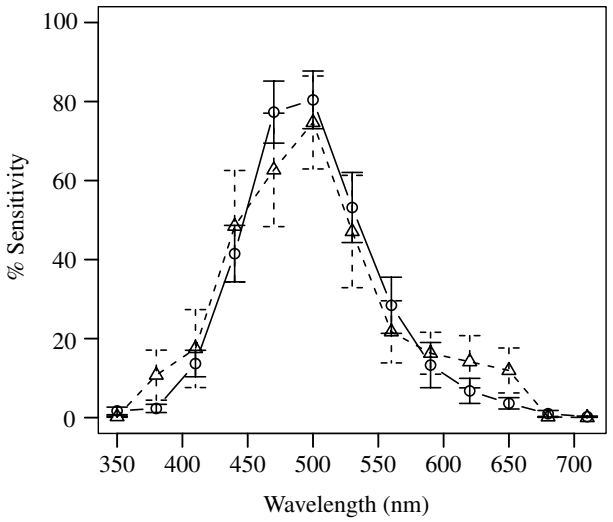

Fig. 6. Mean spectral sensitivity curves for both the lower (solid line, open circles, *N*=14) and the upper (broken line, open triangles, *N*=8) lens eyes (values are means ± 1 s.e.m.). When plotted on the same graph the similarity, in both the peak sensitivity (500 nm) and the shape of the curves, between the two eye types is apparent.

(SSH) and 495 nm (GFRKD), again with similar correlations (0.909, SSH; 0.887, GFRKD).

Removing the β-peak from the GFRKD visual pigment template optimization allows for a much better fit in both eye types (Fig. 8; correlations=0.984, lower eye; 0.968, upper eye). A further increase in goodness of fit can be seen with the addition of self-screening to the model templates (Warrant and Nilsson, 1998). Adding self-screening to the templates requires two additional parameters: k, the absorption coefficient, and l, the length of the photoreceptors. With invertebrate levels of self-screening (k=0.0067 μm^{-1}), the curves are indistinguishable from the no-screening case. However, these fits can be improved further by adding vertebrate level self-screening to the optimization; where k=0.035 μm^{-1}, and l=50 μm for the lower eye photoreceptors and l=35 μm for the upper eye photoreceptors [k-values taken from (Warrant and Nilsson, 1998); l-values from (Nilsson et al., 2005)]. Here, self-screening has the effect of broadening the absorption curve. For the lower eye the half-width increases to 112.1 nm with the addition of screening, compared to 82.0 nm without screening (and without β-peak). For the upper eye the half-width increases to 111.2 nm from 82.8 nm. This results in model half-width values (112 and 111 nm), which are much closer to the data half-width values (107 and 112 nm, respectively). Correspondingly we see a further increase in the correlation values, to 0.991 and 0.980 for the lower and upper eyes, respectively.

Discussion

The underwater world of the mangrove swamp is visually complex. Not only do the roots of the mangrove trees penetrate these shallow waters, but the roots provide purchase for all manner of sessile invertebrates. As a result, the habitat of *Tripedalia cystophora* is filled with mostly vertical obstacles whose surfaces may be sharp, rough, or capable of stinging; all of which are potentially dangerous to the delicate body of a medusa. Still *T. cystophora* navigate this obstacle course with apparent ease, and there is a striking similarity between *T. cystophora* movements and those of the small fish sharing this habitat.

We find that the lens eyes of *T. cystophora* respond over at least 3 log units of light intensities. Similar dynamic ranges are found for the photoreceptors of the hydromedusa *Polyorchis penicillatus* recorded with very similar techniques (Weber, 1982a). Because we have used extracellular mass recordings, it is possible that this range may differ from the dynamic range of a single receptor. However, because our stimulus was adjusted to fill the pupil, we expect a rather homogeneous stimulation of the retina. Also, we know that the photoreceptors of *T. cystophora* have very broad receptive fields (Nilsson et al., 2005) ensuring close to identical stimulation of adjacent receptors. As a result we expect to introduce little or no artifacts from receptors operating at different parts of their response range in the same recording.

Our electrophysiological data support the presence of a single type of opsin molecule in the lens eyes. Nomogram curve-fits to our data based on the SSH rhodopsin template (Stavenga et al., 1993; Warrant and Nilsson, 1998) and the GFRKD template (Govardovskii et al., 2000) indicate that the contribution of a single opsin is sufficient to explain both spectral sensitivity curves (Fig. 7). That opsins are used as the photopigment in cnidarians is also suggested by results from the eyes of the hydromedusae *Polyorchis penicillatus* and *Sarsia tubulosa* (Weber, 1982a; Weber, 1982b). In contrast, another non-bilaterian photo-sensitive system found in the parenchymella larvae of demosponges uses flavins or carotenoids as photopigments (Leys et al., 2002).

Both the SSH and the GFRKD templates describe the presence of an α- and a β-peak in the absorption curve of a visual pigment; both peaks are dictated by the physical chemistry of the visual pigment molecule. The α-peak is defined as the wavelength of maximal light absorption, while the β-peak is always smaller and lies at shorter wavelengths, between 330–360 nm. Importantly, these templates predict the pure responses of opsins, whereas ERGs are affected by filtering, self-screening, and physiology.

In the case of our spectral sensitivity curves, we are unable to fit the β-peak of either template to our data. In fact, if we remove the β-peak from the theoretical template we see a very nice fit between the template and our data (Fig. 8; correlation increases from 0.91 to 0.97). This indicates filtering of short wavelength light, possibly by the lens or tissue covering the lens, which keeps these wavelengths from reaching the retina. It should be noted that the rhopalia are situated on the inner surface of the bell margin (in rhopalial niches) and that light has to pass through the transparent and seemingly colorless bell before it reaches the eyes. Although colorless, the bell probably absorbs UV-light as most living tissue does. Another

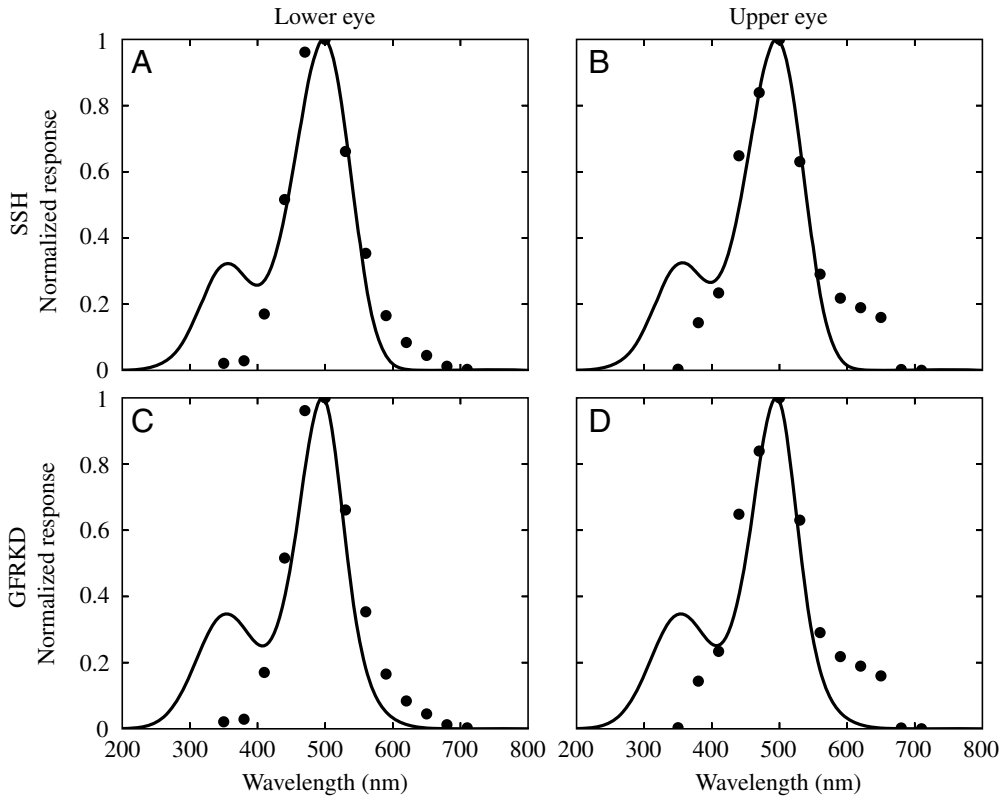

Fig. 7. Spectral sensitivity data (closed circles; A,B) are well modeled by both the SSH rhodopsin template (A,B) and the GFRKD template (described by Govardovskii et al., 2000) (C,D). For the lower eye the models give an α-peak absorbance of 498 nm (A) and 496 nm (C). Both models deviate in the β-peak range and produce similar correlations (0.927, SSH; 0.903, GFRKD). For the upper eye models yield peaks of 496 nm (B) and 495 nm (D), again with similar correlations (0.909, SSH; 0.887, GFRKD).

possibility is that this opsin is not sensitive to UV-light; we find this unlikely given that no other known opsin has such properties.

The fits from both template types were quite similar, but when removing the β-peak from analysis the GFRKD template gave a better fit. Because of the better fit and the extensive data set on which the GFRKD template is based, here and in subsequent analysis we have chosen to focus only on this template.

The templates are based on the absorption curves of the visual pigment molecules themselves, and not on the responses of groups of whole photoreceptor cells as are our data. As a result they fail to take into account the effect of self-screening as light travels along the length of the photoreceptors (Warrant and Nilsson, 1998). Self-screening will have the effect of broadening an absorption curve, because as light travels the length of a photoreceptor, peak-sensitivity wavelengths are preferentially absorbed leaving relatively more non-peak light to be absorbed by the photopigment molecules deeper in the retina.

Self-screening depends on two parameters: l, the length of the photoreceptor, and k, the absorption coefficient of the photoreceptor. In our case we know l from our anatomical model of the lens eyes (Nilsson et al., 2005). k is not known for *T. cystophora* or from other cnidarians; however, k is known from several invertebrates and vertebrates [for summary of k-values see Warrant and Nilsson (Warrant and Nilsson, 1998)]. Using a typical invertebrate value, k=0.0067 μm^{-1} (Bruno et al., 1977), and a typical vertebrate value, k=0.035 μm^{-1} (Partridge, 1990), we have added self-screening to our template fits (Fig. 8). Here we see no appreciable difference with the invertebrate k-value. However, self-screening broadens and improves the fits with the vertebrate value of k. Although cubomedusae are most definitely invertebrates, their photoreceptors are not the typical rhabdomeric photoreceptors found among invertebrates. Nor are they the typical vertebrate ciliary type, with photopigment packed in lamellar disks – their receptive outer segments extend from a central cilium, much like that of vertebrate photoreceptors, but their photopigment is packed in microvilli (Yamasu and Yoshida, 1976). Still, it is possible that this cilium–microvilli arrangement allows for denser packing of photopigment, and therefore higher k-values, than the typical rhabdomeric microvilli arrangement of most invertebrates.

There is another possible explanation for broadening of the spectral sensitivity curves apart from self-screening; broadening due to the presence of additional opsins with different α-peaks. Again, because of the nature of extracellular recordings we are recording from multiple receptors simultaneously in our experiments. If some of these receptors contained different opsins, each would contribute to the recorded response. Adding a second opsin to the template fitting will always result in stronger correlations; this is particularly true in the case of the upper eye, which has somewhat of a long wavelength shoulder. However, the single opsin correlations are so good that the contribution of any putative second opsin to the sensitivity curve must be small. We find it most likely that the examined eyes have a single

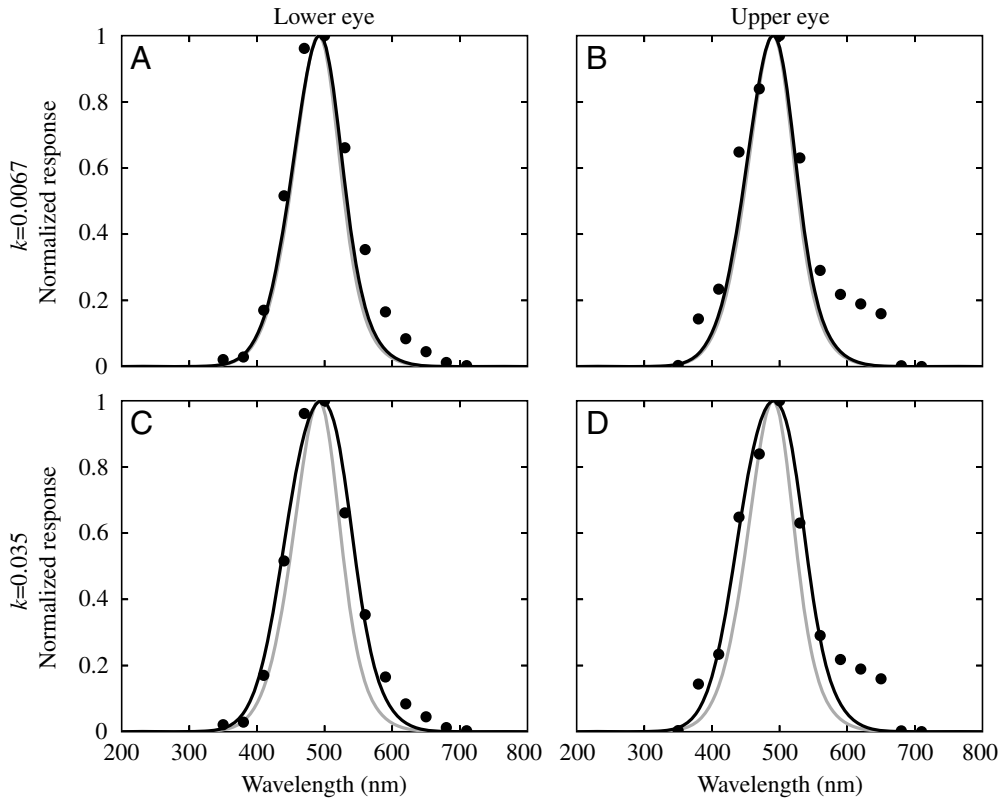

Fig. 8. Removing the β-peak from the GFRKD visual pigment template optimization allows for a much better fit in both eye types (gray lines; correlations=0.984, lower eye; 0.968, upper eye). With invertebrate levels of self-screening (k=0.0067; A,B, black lines) the curves are indistinguishable from the no screening case (A,B, gray lines). However, these fits can be improved further by adding vertebrate level self-screening to the optimization (C,D, black lines); where k= 0.035 μm^{-1}, and l=50 μm for the lower eye photoreceptors and l=35 μm for the upper eye photoreceptors. Here, self-screening has the effect of broadening the absorption curve. For the lower eye (C) the half-width increases to 112.1 nm with the addition of screening, compared to 82.0 nm without screening. For the upper eye (D) the half-width increases to 111.2 nm from 82.8 nm. Correspondingly the correlation values increase to 0.991 and 0.980 for the lower and upper eyes, respectively.

photoreceptor population, containing a single type of opsin. If a second population of photoreceptor, with a second type of opsin is present, it is extremely rare in the area of the retina from which we recorded.

If indeed the lens eyes contain only a single type of opsin, then these eyes will not provide *T. cystophora* with color vision. Color vision is thought to be useful for animals living near the surface of the water. Ripples at the water surface create a lensing effect and focus incident light in a temporally changing pattern (Snyder and Dera, 1970). Color vision has been shown to enhance contrast detection under these circumstances by minimizing the dependence on intensity (Maximov, 2000). Without such compensation, detection of objects can be difficult in this light environment. *T. cystophora* does not seem to require this strategy and may rely on other filters, such as temporal or spatial low pass filters, to remove this flicker.

Light in the mangrove waters is relatively green (Lythgoe, 1979), but peak spectral sensitivity in both lens eyes falls more towards blue–green. The upper eyes point upward (Berger, 1898) (M.M.C. and D.-E.N., unpublished data), toward the surface of the water, and therefore gather light that comes through Snell's window (Lythgoe, 1979). Medusae are normally found within 10 cm of the surface during the day; if they were in the open water the light coming through Snell's window would contain most of the full spectrum of sunlight (Partridge, 1990). However, medusae are only found under or just at the edge of the mangrove canopy (never in the open channels between the mangrove islands), so a large part of the upper eye visual field consists of green leaves. The slightly blue bias of their spectral sensitivity may help improve contrast (Lythgoe, 1979; Partridge, 1990).

The lower eyes also experience a predominantly green environment because, although they point horizontally and downward, these nearshore, shallow waters are rich with algae and other organic materials (Lythgoe, 1979). Here again sensitivity to blue–green light will help increase contrast in the visual scene. Spectral analysis of the natural habitat of *T. cystophora* is necessary to further explore this result. It is worth noting that the spectral sensitivities reported here agree well with behavioral responses where medusae are attracted to blue or green light shafts, but ignore the red (Coates, 2005).

Vision is an ideal sense for judging objects, like mangrove roots, at a distance. Vision allows accurate evaluation of the mangrove environment, and the obstacles present there at a safe distance, all necessary for navigating this habitat. However, useful vision requires eyes that are tailored to gather the appropriate information. We have recently published data on the spatial resolution of the lens eyes of *Tripedalia cystophora* and we found them to perform strong low-pass spatial filtering, leaving only large objects (like prop roots) to be seen (Nilsson et al., 2005). In the present study, we have shown that these eyes do indeed respond physiologically to light stimuli with properties that appear suited to their visual environment. Their spectral sensitivity is consistent with a vitamin A-1 based opsin molecule with a blue–green peak sensitivity that should optimize contrast in their predominantly green world. Further, in spite of the immunoreactivity to several visual pigments

found by Martin (Martin, 2004), our results suggest the presence of a single opsin only. The long wavelength shoulder found in the upper lens eye could be due to the presence of an additional opsin, but if so it would be rare in the part of the eye we recorded from. This possibility could be resolved in the future by selective adaptation experiments. [It should also be noted here that Martin worked on a different species, *Carybdea marsupialis* (Martin, 2004).] In the case of a single opsin we know that color vision will not be involved in the visual tasks of the lens eyes and that these eyes are likely involved in only colorblind visual tasks, such as motion vision. Obstacle avoidance seems to be an important task for these organisms and this requires the visual detection of flow fields only and not any more complicated visual tasks such as object recognition (Tammero and Dickinson, 2002). It seems that the lens eyes of *Tripedalia cystophora*, and presumably also other cubomedusae, could be the sensory base for their excellent obstacle avoidance by way of motion detection (see supplementary material for a video of *T. cystophora* navigating their mangrove environment).

We are grateful for the careful critiques of the two anonymous reviewers and to Dr Christian Reilly for shipping animals from California to Sweden. We also thank our various funding agencies: M.M.C. acknowledges the support of the NSF predoctoral fellowship program, and especially the travel funds to facilitate international collaboration; A.G. acknowledges grant 21-04-0423 from the Danish Research Council; D.-E.N. the continued support of the Swedish Research Council.

References

Berger, E. W. (1898). The histological structure of the eyes of cubomedusae. *J. Comp. Neurol.* **8**, 223-230.

Berger, E. W. (1900). Physiology and histology of the Cubomedusae, including Dr F. S. Conant's notes on the physiology. *Mem. Biol. Lab. Johns Hopkins Univ.* **IV**, 1-84.

Bruno, M. S., Barnes, S. N. and Goldsmith, T. H. (1977). The visual pigment and visual cycle of the lobster Homarus. *J. Comp. Physiol.* **120**, 123-142.

Buskey, E. J. (2003). Behavioral adaptations of the cubozoan medusa *Tripedalia cystophora* for feeding on copepod (*Dioithona oculata*) swarms. *Mar. Biol.* **142**, 225-232.

Claus, C. (1878). Ueber *Charybdea marsupialis*. *Arb. Zool. Inst. Univ. Wien* **II**, 16-55.

Coates, M. M. (2003). Visual ecology and functional morphology of the Cubozoa. *Integr. Comp. Biol.* **43**, 542-548.

Coates, M. M. (2005). Vision in a cubozoan jellyfish, *Tripedalia cystophora*. PhD dissertation, Stanford University, Stanford, USA.

Govardovskii, V. I., Fyhrquist, N., Reuter, T., Kuzmin, D. and Donner, K. (2000). In search of the visual pigment template. *Vis. Neurosci.* **17**, 509-528.

Greve, W. (1968). The 'planktonkreisel', a new device for culturing zooplankton. *Mar. Biol.* **1**, 201-203.

Hamner, W. M., Jones, M. S. and Hamner, P. P. (1995). Swimming, feeding, circulation, and vision in the Australian box jellyfish, *Chironex fleckeri* (Cnidaria:Cubozoa). *Mar. Freshw. Res.* **46**, 985-990.

Land, M. F. (1981). Optics and vision in invertebrates. In *Comparative Physiology and Evolution of Vision in Invertebrates, Handbook of Sensory Physiology.* Vol. II/6B (ed. H. Autrum), pp. 471-592. Berlin: Springer.

Laska, G. and Hündgen, M. (1982). Morphologie und ultrastruktur der lichtsinnesorgane von *Tripedalia cystophora* Conant (Cnidaria, Cubozoa). *Zool. Jb. Anat.* **108**, 107-123.

Leys, S. P., Cronin, T. W., Degnan, B. M. and Marshall, J. N. (2002). Spectral sensitivity in a sponge larva. *J. Comp. Physiol. A* **188**, 199-202.

Livingstone, M. S. and Huebel, D. H. (1986). Psychophysical evidence for separate channels for the perception of form, color, movement, and depth. *J. Neurosci.* **7**, 3416-3468.

Lythgoe, J. N. (1979). *The Ecology of Vision*. Oxford: Clarendon Press.

Mackie, G. O. (1999). Coelenterate organs. *Mar. Freshw. Behav. Physiol.* **32**, 113-127.

Martin, V. J. (2004). Photoreceptors of cubozoan jellyfish. *Hydrobiologia* **530-531**, 135-144.

Maximov, V. V. (2000). Environmental factors which may have led to the appearance of colour vision. *Philos. Trans. R. Soc. Lond. B* **355**, 1239-1242.

Nilsson, D.-E. and Howard, J. (1989). Intensity and polarization of the eyeshine in butterflies. *J. Comp. Physiol. A* **166**, 51-56.

Nilsson, D.-E., Gislén, L., Coates, M. M., Skogh, C. and Garm, A. (2005). Advanced optics in a jellyfish eye. *Nature* **435**, 201-205.

Parkefelt, L., Nilsson, D.-E. and Ekström, P. (2005). A bilaterally symmetric nervous system in the rhopalia of a radially symmetric cubomedusa. *J. Comp. Neurol.* **492**, 251-262.

Partridge, J. C. (1990). The colour sensitivity and vision of fishes. In *Light and Life in the Sea* (ed. P. J. Herring, A. K. Campbell, M. Whitfield and L. Maddock), pp. 167-184. Cambridge: Cambridge University Press.

Pearse, J. S. and Pearse, V. B. (1978). Vision in cubomedusan jellyfishes. *Science* **199**, 458.

Piatigorsky, J., Horwitz, J., Kuwabara, T. and Cutress, C. E. (1989). The cellular eye lens and crystallins of cubomedusan jellyfish. *J. Comp. Physiol. A* **164**, 577-587.

Raskoff, K. A., Sommer, F. A., Hamner, W. M. and Cross, K. M. (2003). Collection and culture techniques for gelatinous zooplankton. *Biol. Bull. Mar. Biol. Lab. Woods Hole* **204**, 68-80.

Snyder, R. L. and Dera, J. (1970). Wave-induced light-field fluctuations in the sea. *J. Opt. Soc. Am.* **60**, 1072-1079.

Stavenga, D. G., Smits, R. P. and Hoenders, B. J. (1993). Simple exponential functions describing the absorbance bands of visual pigment spectra. *Vision Res.* **33**, 1011-1017.

Stewart, S. E. (1996). Field behavior of *Tripedalia cystophora* (Class Cubozoa). *Mar. Freshw. Behav. Physiol.* **27**, 175-188.

Tammero, L. F. and Dickinson, M. H. (2002). The influence of visual landscape on the free flight behavior of the fruit fly *Drosophila melanogaster*. *J. Exp. Biol.* **205**, 327-343.

Warrant, E. J. and Nilsson, D.-E. (1998). Absorption of white light in photoreceptors. *Vision Res.* **38**, 195-207.

Weber, C. (1982a). Electrical activities of a type of electroretinogram recorded from the ocellus of a jellyfish, *Polyorchis penicillatus* (Hydromedusae). *J. Exp. Zool*. **223**, 231-343.

Weber, C. (1982b). Electrical activity in response to light of the ocellus of the hydromedusan, *Sarsia tubulosa*. *Biol. Bull. Mar. Biol. Lab. Woods Hole* **162**, 413-422.

Yamasu, T. and Yoshida, M. (1976). Fine structure of complex ocelli of a cubomedusan, *Tamoya bursaria* Haeckel. *Cell Tissue Res.* **170**, 325-339.